Simulation of dispersed two-phase flow using a coupled Volume-of-Fluid/Level-Set method

By E.R.A. Coyajee†, M. Herrmann AND B.J. Boersma†

In this paper, a coupled Volume-of Fluid/Level-Set interface advection method is considered for the simulation of incompressible two-phase flow. With this method, mass conservation for both phases can be achieved up to specified tolerance in each computational cell. Representation of surface tension forces, however, is found unsatisfactory for the stationary droplet (Laplace) problem, as the procedure to couple the Volume-of-Fluid (VOF) and Level-Set (LS) functions gives rise to increased levels of spurious currents. An attempt to improve the coupling of VOF and LS interface descriptions is reported.

1. Introduction

In many industrial flows, the size distribution of drops in a liquid dispersion is of primary importance to process performance. The size distribution is governed by continuous break-up and coalescence of the dispersed phase. In contrast to break-up, coalescence requires the interaction of multiple droplets. In the past, several studies of droplet interaction have been conducted, e.g. Wang, Zinchenko & Davis (1994) and Loewenberg & Hinch (1997). Most of these studies are performed in the limiting condition of Stokes flow, i.e. occurring in emulsification and polymer blending processes. However, industrial flows are frequently turbulent. In this case, if the droplet Reynolds number is finite, the interaction of droplets and coalescence probability is expected to be influenced by effects of inertia in the flow.

To perform a detailed investigation of the behavior of multiple droplets in an incompressible flow at finite droplet Reynolds number, we aim to apply an appropriate numerical method. In this work, the mass conserving Level-Set (MCLS) method introduced by Van der Pijl, Segal, Vuik & Wesseling (2004) is considered for the simulation of two-phase flows. In the MCLS method, the interface between both fluids is advected by a combined VOF/LS approach, with the purpose of eliminating drawbacks of the individual methods by combining advantages.

1.1. *VOF method*

In the VOF method the interface is represented implicitly on a fixed grid by a marker function, commonly denoted ψ. Indicating the fractional volume of one of the fluids, the VOF function in a computational cell, Ω, is defined from:

$$\psi = \frac{\int_\Omega \chi d\Omega}{\int_\Omega d\Omega}, \tag{1.1}$$

where χ is the characteristic function, i.e. $\chi = 1$ in one fluid and $\chi = 0$ in the other fluid. The value of the VOF function is $0 < \psi < 1$ for cells which are cut by the interface and 0 or 1 elsewhere.

† J.M. Burgerscenter, Laboratory for Aero and Hydrodynamics, Delft University of Technology, Leeghwaterstraat 21, 2628 CA Delft, The Netherlands.

The main advantage of the VOF method is that interface advection can be performed such that the volume or mass of each phase is conserved. On the other hand, the location of the interface is not explicitly defined by the VOF function. Consequently, geometric reconstruction of the interface (or its normal) has to be performed for advection or the computation of curvature. Over the past years, reconstruction procedures have been advanced from Simple Linear Interface Construction up to Piecewise Linear Interface Construction and even piecewise parabolic approximations in Renardy & Renardy (2002). Therefore, computation of interface normals and curvature have improved considerably. The reconstruction procedures themselves however have become complex and their implementation elaborate.

1.2. *LS method*

An LS approach for simulation of two-phase flow has been introduced by Sussman, Smereka & Osher (1994). In the LS methodology, the interface is represented implicitly on a fixed grid by the zero-level of a marker function, commonly denoted ϕ, i.e. $\phi = 0$ at the interface. Away from the interface, the marker function is required to be a distance function, i.e. $\phi < 0$ in phase '1' and $\phi > 0$ in phase '2'. Using the distance function property, the discontinuous surface tension force and discontinuous phase variables such as viscosity and density are easily regularized and implemented according to the Continuous Surface Force methodology (Brackbill, Kothe & Zemach 1992).

Advection of the interface is performed by advecting the LS function as if it were a material property:

$$\frac{\partial \phi}{\partial t} + \mathbf{u} \cdot \nabla \phi = 0. \tag{1.2}$$

For the numerical solution of equation 1.2, straightforward methods for hyperbolic conservation laws are applied, which are diffusive. The diffusion changes the volume enclosed by $\phi = 0$, causing transport of mass from one phase to another. For the current objective, long-term computation of dispersed flow, mass losses would result in unacceptable changes in the properties of droplets and their behavior.

1.3. *MCLS method*

To overcome the problem of mass diffusion in the LS method, the MCLS method combines both LS and VOF approaches: The LS methodology is used for representation of the interface, while the VOF methodology is used for volume preserving advection of both phases. Such a combined approach requires methods to switch between LS and VOF interface descriptions. The MCLS method uses the following relation introduced in the coupled LS/VOF (CLSVOF) method by Sussman & Puckett (2000):

$$\psi = \frac{\int_\Omega H(\phi) d\Omega}{\int_\Omega d\Omega}, \tag{1.3}$$

where $H(\phi)$ is the Heaviside function, defined

$$H(\phi) = \begin{cases} 1 & \text{if } \phi > 0 \\ 0 & \text{otherwise.} \end{cases} \tag{1.4}$$

Using equation 1.3 and assuming a piecewise linear interface in each computational cell, Van der Pijl, Segal & Vuik (2004) propose an explicit relation between ψ and ϕ of the form:

$$\psi = f(\phi, \nabla \phi), \tag{1.5}$$

which will be discussed further in section 3.2. In addition to equation 1.5, a coupled VOF/LS method requires a way of computing ϕ from ψ. However, no explicit inverse relation of equation 1.5 seems to be available. Instead, an iterative procedure is performed to correct an approximate solution of the LS function. Unfortunately, our tests indicate that the corrections give rise to enhancement of the so-called spurious currents in the stationary bubble problem. Therefore this work tries to make a contribution to improve the coupling between LS and VOF interface representations.

The organization of this article is as follows. In the next section a set of equations is presented for the description of multiphase flow. Subsequently in section 3, the numerical method of Van der Pijl, Segal & Vuik (2004) is presented, with specific emphasis on the inverse coupling between the LS and VOF function. In section 4, results are presented for the stationary droplet problem. Furthermore, an analysis and proposition for improvement of the VOF/LS coupling in the MCLS method is given, followed by the results of a number of test cases. A discussion concludes the paper.

2. Governing equations

Multiphase flow is described by a set of equations for fluid and interface motion. The motion of the fluids is described by the Navier-Stokes (NS) equations:

$$\rho(\phi)\left(\frac{\partial \mathbf{u}}{\partial t} + \mathbf{u}\cdot\nabla\mathbf{u}\right) = -\nabla p + \nabla\cdot\left(\mu(\phi)\left(\nabla\mathbf{u} + (\nabla\mathbf{u})^T\right)\right) + \mathbf{f} \tag{2.1}$$

and the continuity equation for incompressible flow:

$$\nabla\cdot\mathbf{u} = 0. \tag{2.2}$$

The motion of the interface is described by the following equations for the LS:

$$\frac{\partial \phi}{\partial t} + \mathbf{u}\cdot\nabla\phi = 0 \tag{2.3}$$

and VOF function:

$$\frac{\partial \psi}{\partial t} + \mathbf{u}\cdot\nabla\psi = 0. \tag{2.4}$$

In equation 2.1, ρ, μ, p, $\mathbf{u} = (u, v, w)^T$ and $\mathbf{f}$ respectively represent density, viscosity, pressure, the velocity vector and a volume force. The volume force $\mathbf{f}$ may represent gravity as well as surface tension forces. A continuum description of the discontinuous surface tension force acting at the interface between two fluids:

$$\sigma\kappa(\phi)\nabla H(\phi) \tag{2.5}$$

was introduced by Brackbill, Kothe & Zemach (1992) and cast into LS methodology by Chang, Hou, Merriman & Osher(1996). Here, $\kappa(\phi)$ is the mean curvature, defined from:

$$\kappa(\phi) = \nabla\cdot\frac{\nabla\phi}{|\nabla\phi|}. \tag{2.6}$$

Density $\rho(\phi)$ and viscosity $\mu(\phi)$ are allowed to vary between phase '1' or '2', and are defined:

$$\mu(\phi) = \mu_1\left(1 - H(\phi)\right) + \mu_2 H(\phi), \tag{2.7}$$

$$\rho(\phi) = \rho_1\left(1 - H(\phi)\right) + \rho_2 H(\phi). \tag{2.8}$$

3. Numerical method

In the method of Van der Pijl, Segal & Vuik (2004), the computational domain is a 3D rectangular box. Equations 2.1-2.4 are spatially discretized on a uniform Cartesian mesh. A standard staggered arrangement of variables is used, i.e. velocity components are located on the cell faces, whereas pressure, density, VOF and LS variables are defined at cell centers.

Although the original method allows unequal densities in either phase, in this report only fluids of equal density are considered as our focus is on the effects of the VOF/LS coupling on computation of surface tension. The coupling itself is in no way influenced by the density ratio, and for further details about the implementation of discontinuous density we refer to Van der Pijl, Segal, Vuik & Wesseling (2004).

A single time-step in our code consists of the following sequence. First, for a given interface position (i.e. LS function), the flow field is advanced to obtain the velocity at the new time level. Second, given the velocity, the interface is advected to obtain a new interface position (i.e. LS function).

3.1. *Fluid flow*

Time integration of equations 2.1 and 2.2 is performed with the second order Adams-Bashforth method in the framework of a pressure correction method. Rewriting equation 2.1 into

$$\frac{\partial \mathbf{u}}{\partial t} = \mathbf{f}\left(\mathbf{u}, \phi\right) - \nabla \tilde{p}, \tag{3.1}$$

where $\tilde{p} = p/\rho$ denotes the reduced pressure, the integration scheme is given from:

$$\frac{\mathbf{u}^* - \mathbf{u}^n}{\Delta t} = \frac{3}{2}\left(\mathbf{f}(\phi^n, \mathbf{u}^n)\right) - \frac{1}{2}\left(\mathbf{f}(\phi^{n-1}, \mathbf{u}^{n-1})\right) + \nabla \tilde{p}^{n-1/2}, \tag{3.2}$$

$$\nabla^2 \tilde{p}^* = \frac{1}{\Delta t} \nabla \cdot \mathbf{u}^*, \tag{3.3}$$

$$\nabla \tilde{p}^{n+1/2} = \nabla \tilde{p}^{n-1/2} + \nabla \tilde{p}^*, \tag{3.4}$$

$$\mathbf{u}^{n+1} = \mathbf{u}^* - \Delta t \nabla \tilde{p}^*. \tag{3.5}$$

Due to the assumption of uniform density, we can use a direct Poisson solver to obtain the pressure from equation 3.3, making the code very efficient. For spatial discretization of equations 2.1 and 2.2, central second order finite differences are used. Finally, the following regularized Heaviside function is used for the computation of the surface tension volume force.:

$$H_\alpha(\phi) = \begin{cases} 0 & \text{if } \phi < -\alpha \\ \frac{1}{2}\left(1 + \frac{\phi}{\alpha} + \frac{1}{\pi}\sin(\pi\phi/\alpha)\right) & \text{if } |\phi| \leq \alpha \\ 1 & \text{if } \phi > \alpha \end{cases}, \tag{3.6}$$

where α is chosen as $\alpha = 3/2$.

3.2. *Interface advection*

The interface advection procedure in the MCLS method is the following:

1. Given ϕ^n, compute ψ^n;
2. Advect ψ^n toward ψ^{n+1};
3. Advect ϕ^n toward ϕ^*;

4. Correct ϕ^* to obtain ϕ^{n+1}, such that $|\psi^{n+1} - f(\phi^{n+1}, \nabla\phi^{n+1})| < \epsilon$ in each computational cell.

This procedure will be explained in the following sections.

3.2.1. *Computation of VOF from the LS function*

As discussed in the introduction, a direct relation is used to compute the VOF from the LS function in 3D:

$$\psi = f\left(\phi, \nabla\phi\right). \tag{3.7}$$

In the MCLS method, the interface is assumed to be piecewise linear in each computational cell. As a consequence, the interface is a 2D plane, which can be described by a normal vector and a distance to some position along the normal direction. The normal to the interface is simply described by:

$$\mathbf{n} = \frac{\nabla\phi}{|\nabla\phi|} \approx \nabla\phi \tag{3.8}$$

as the LS function is maintained a distance function in our computations (see section 3.2.3), for which $|\nabla\phi| \equiv 1$. In the actual implementation, $\nabla\phi$ is estimated using central second order finite differences. The description of the interface is completed by the local value of the LS function, describing the distance between the interface and the cell center.

With the assumption of a piecewise linear interface, equation 1.3 is simplified to:

$$\psi = \frac{\int_{\Omega_k} H(\phi_k + \nabla\phi_k \cdot (\mathbf{x} - \mathbf{x}_k))\, d\Omega}{\int_{\Omega_k} d\Omega}, \tag{3.9}$$

where ϕ_k and $\nabla\phi_k$ are the discrete values of the LS function and its gradient in a computational cell, Ω_k, and $\mathbf{x}_k$ denotes the position of the cell center. Now, at the piecewise linear interface, described by the local values ϕ_k and $\nabla\phi_k$, the value of the LS function is known: $\phi = 0$. Then, from the location of the planar interface and the local gradient of the LS function, any distance between the interface and the faces of the computational cell can be computed. Therefore, it is possible to determine the VOF value in a computational cell from a geometric computation of the volume for which $H(\phi) = 1$, in accordance with equation 1.3. For the complete mathematical formulation of equation 3.8, we refer to Van der Pijl, Segal & Vuik (2004).

3.2.2. *VOF advection*

The VOF advection is performed by means of an operator-split method. To this aim, equation 2.4 is rewritten into:

$$\begin{aligned}
\frac{\partial\psi}{\partial t} + \frac{\partial(u\psi)}{\partial x} &= \psi\frac{\partial u}{\partial x} \\
\frac{\partial\psi}{\partial t} + \frac{\partial(v\psi)}{\partial y} &= \psi\frac{\partial v}{\partial y} \\
\frac{\partial\psi}{\partial t} + \frac{\partial(w\psi)}{\partial z} &= \psi\frac{\partial w}{\partial z}.
\end{aligned} \tag{3.10}$$

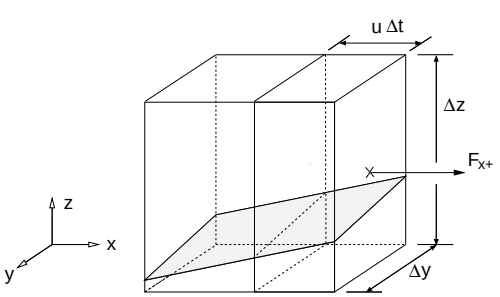

FIGURE 1. Computational cell with flux F_{x+} and its donating region $u\Delta t\Delta y\Delta z$. The interface is indicated by a patterned surface.

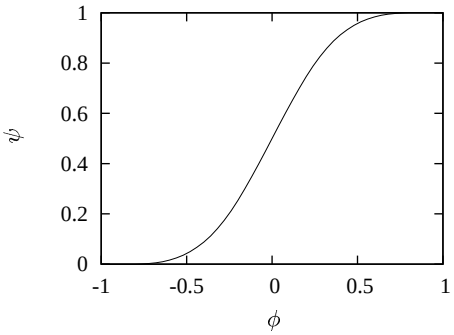

FIGURE 2. Graph of the relation between ϕ and ψ for $\nabla\phi = \left(\frac{1}{3}\sqrt{3}, \frac{1}{3}\sqrt{3}, \frac{1}{3}\sqrt{3}\right)$.

A conservative numerical approximation of equation 3.10 is obtained by considering fluxes of fluid, denoted F, flowing through the boundary of a cell during time-step Δt:

$$\begin{aligned}
\frac{\psi^* - \psi^n}{\Delta t} &= -\frac{F^n_{x+} - F^n_{x-}}{\Delta x\Delta y\Delta z\Delta t} + \psi^* \frac{u_+ - u_-}{\Delta x} \\
\frac{\psi^{**} - \psi^*}{\Delta t} &= -\frac{F^*_{y+} - F^*_{y-}}{\Delta x\Delta y\Delta z\Delta t} + \psi^{**} \frac{v_+ - v_-}{\Delta y} \\
\frac{\psi^{***} - \psi^{**}}{\Delta t} &= -\frac{F^{**}_{z+} - F^{**}_{z-}}{\Delta x\Delta y\Delta z\Delta t} + \psi^{***} \frac{w_+ - w_-}{\Delta z} \\
\frac{\psi^{n+1} - \psi^{***}}{\Delta t} &= -\psi^* \frac{u_+ - u_-}{\Delta x} - \psi^{**} \frac{v_+ - v_-}{\Delta y} - \psi^{***} \frac{w_+ - w_-}{\Delta z},
\end{aligned} \tag{3.11}$$

where subscripts indicate the corresponding face of a cell. The discrete flux is defined:

$$F = \int_{\Omega_D} H(\phi) d\Omega, \tag{3.12}$$

where Ω_D is the donating region, which contains the fluid that will flow through a face during a time-step Δt. An example of a discrete flux, F_{x+}, and its donating region is displayed in figure 1. To compute the magnitude of the particular flux in figure 1, the VOF within the donating region of size: $u\Delta t\Delta y\Delta z$ needs to be considered. To compute the discrete fluxes, equation 3.7 can be used as its formulation enables the computation of a fluid fraction in any rectangular domain.

3.2.3. *LS advection*

As a final step in the interface advection procedure one would like to obtain ϕ^{n+1} from ψ^{n+1} directly. Unfortunately, no explicit inverse relation of equation 3.7 appears to be available and a different strategy needs to be applied. Although interface advection of the LS function is not preferred as the solutions are not strictly mass conserving, ϕ^n can be advected to obtain an approximate solution of the LS function.

The preliminary update of the LS function, denoted ϕ^*, is obtained by solving equation 2.3. Subsequently, reinitialization is performed to keep the LS function a distance function as in Sussman, Smereka & Osher (1994). First order discretization is used for both advection and reinitialization procedures. Obviously, first order methods suffer from considerable numerical diffusion, resulting in transport of mass from one phase to an-

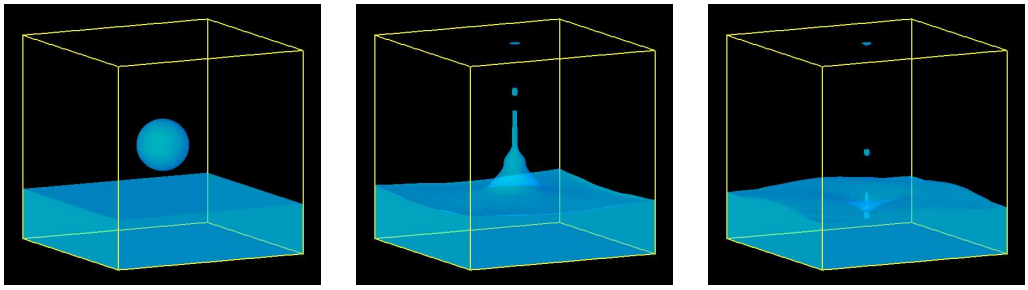

FIGURE 3. Droplet falling into a free surface. Simulation of an air-water flow without surface tension. Courtesy of Sander van der Pijl.

other. However, as mass conservation is ensured by the correction procedure described in the next section, Van der Pijl, Segal, Vuik & Wesseling (2004) argue in favor of a low order method because the diffusion provides a smooth approximate solution for the LS function.

3.2.4. *Correction of the LS function*

Finally, ϕ^* is corrected, providing a solution ϕ^{n+1} which satisfies:

$$|\psi_k^{n+1} - f(\phi_k^{n+1}, \nabla\phi_k^{n+1})| \leq \epsilon \quad \forall \quad k = 1, 2, \ldots, K \tag{3.13}$$

where K is the total number of computational cells and ϵ a tolerance. In this work we use $\epsilon = 1 \cdot 10^{-4}$.

The main idea of the correction procedure is as follows: Keeping $\nabla\phi$ at a constant value, the interface equation 3.7 gives a one-to-one relation between the LS and VOF function:

$$\phi = g(\psi, \nabla\phi). \tag{3.14}$$

Figure 2 shows an example of the graph of such a relation between the LS and VOF function for $\nabla\phi = \left(\frac{1}{3}\sqrt{3}, \frac{1}{3}\sqrt{3}, \frac{1}{3}\sqrt{3}\right)$. From figure 2 it will be clear that, while assuming a constant gradient of the LS function, the local value of the LS function in a cell can be adjusted such that the required local value of the VOF function is obtained. We found this procedure similar to the one in Sussman & Puckett (2000), in which a linearly constructed piece of interface is shifted along its normal direction to minimize a mass error. Here, the assumption of a constant gradient is equivalent to solving a linearized problem.

Using equation 3.14, the following iterative procedure is executed to correct the preliminary LS function:

- $\phi^0 = \phi^*$;
- $\delta\psi_k = |\psi_k^{n+1} - f(\phi_k^0, \nabla\phi_k^0)|$;
- Repeat until $\delta\psi_k < \epsilon \; \forall k$

  $$\phi_k^{m+1} = \begin{cases} g(\psi_k^{n+1}, \nabla\phi_k^m) & \text{if } \delta\psi_k > \epsilon \\ \phi_k^m & \text{if } \delta\psi_k < \epsilon; \end{cases}$$

  $\delta\psi_k = |\psi_k^{n+1} - f(\phi_k^{m+1}, \nabla\phi_k^{m+1})|$;
- $\phi^{n+1} = \phi^{m+1}$.

Case	1	2	3	4	5	6	7	8	9	10	11	12
σ	1	0.1	0.01	0.001	1	0.1	0.01	0.001	1	0.1	0.01	0.001
μ	1	1	1	1	0.1	0.1	0.1	0.1	0.01	0.01	0.01	0.01

TABLE 1. Parameter combinations of surface tension σ and viscosity μ for the Laplace problem.

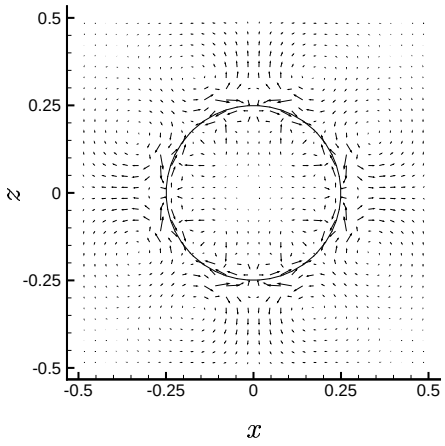

FIGURE 4. Laplace problem: Velocity vectors and interface over a cross-section ($y = 0$) of the droplet at time $t = 0.1$. MCLS method used for case 7 with $h = 1/32$.

4. Results

Figure 3 shows three images of a simulation of a droplet falling into a free surface. The maximum relative mass error during this computation is less than $1.6 \cdot 10^{-4}$. Considering the complexity of the interface motion, this result clearly shows the capability of the MCLS method to conserve mass. Nevertheless, the simulation of figure 3 is performed without the surface tension force in equation 2.1. To investigate the surface tension representation in the MCLS method, the Laplace or stationary droplet problem is simulated in this section.

4.1. *Laplace problem*

The Laplace or stationary bubble/droplet problem is considered an important test case for implementation of surface tension forces (Renardy & Renardy 2002). Here, the Laplace problem is simulated in a computational domain of dimensions $1 \times 1 \times 1$. Boundary conditions are periodic in all directions. Initial conditions are $\mathbf{u} = (0, 0, 0)$ for the fluid velocity and $R_b = 0.25$ for the radius of the droplet. Computations have been performed using $\rho = 1$ and various combinations of σ and μ, listed in table 1. For a grid refinement study, uniform meshes are used with $h = 1/16, 1/32, 1/64, 1/128$. The time-step is $\Delta t = 2 \cdot 10^{-5}$. In the simulations, the magnitude of the parasitic currents is monitored by measuring

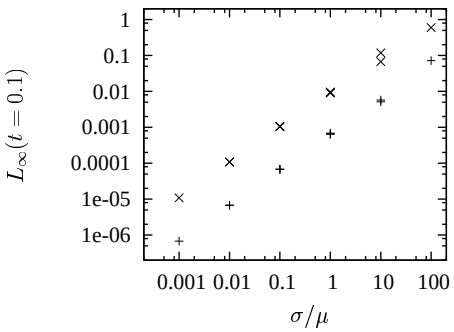

FIGURE 5. Laplace problem: Results of the parameter study for the MCLS method (×) compared to LS advection (+), $h = 1/64$.

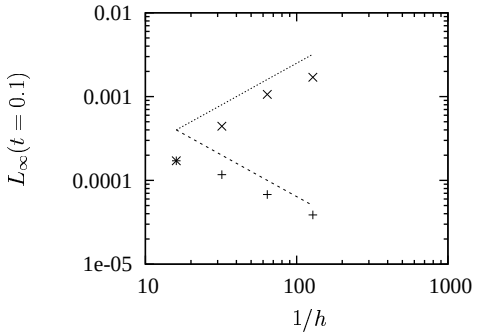

FIGURE 6. Laplace problem: Results of a grid refinement test for the MCLS method (×) compared to LS advection (+), for case 7. (. . .) Line of slope +1. (− −) Line of slope −1.

the maximum norm of the error in velocity, defined from†:

$$L_\infty = \max_{1 \le k \le K} (|u|_k, |v|_k, |w|_k). \tag{4.1}$$

Simulations have been run for all mesh sizes and combinations of parameters up to $t = 0.1$. At this time, the spurious or parasitic currents (displayed in figure 4) are found to have saturated toward a maximum level. This behavior is similar to the behavior found in Renardy & Renardy (2002). Also in accordance with other authors we find that $L_\infty(t = 0.1)$ increases linearly with the ratio σ/μ (figure 5). Nonetheless, the spurious currents seem rather high. To compare, we have recalculated all cases using only first order LS advection, i.e. disregarding the coupling between the advected VOF and LS functions in the simulation. The results are also given in figure 5 and reveal lower levels of parasitic currents.

From the comparison of results of the LS and MCLS methods, we conjecture the enhancement of spurious currents is caused by the inverse coupling between the LS and VOF functions. In the procedure of section 3.2.4, corrections are only introduced in cells where the local mass error is larger than a certain tolerance. As the corrections are only applied locally, problems may arise in the computation of curvature which involves second order derivatives of the LS function. We have done an analysis of a singular perturbation in ϕ on the curvature, i.e. introducing $\phi = \phi(\mathbf{x}) + \varepsilon$ to the discretized curvature $\kappa(\phi)$. For a singular perturbation $\varepsilon = O(h)$, the resulting error in curvature is found to be $O(1/h)$.

The previous analysis, which suggests that the corrections act as a singular perturbation on the smooth initial LS function, is confirmed by the results of our simulations. Figure 6 shows results of a grid refinement study of the maximum norm for case 7, both for LS advection and the MCLS method. The magnitude of the spurious currents in the MCLS method is found to increase approximately proportional with $1/h$, whereas first order convergence is found for LS advection‡.

† Note that, since the exact solution for the fluid velocity in the Laplace problem is zero velocity everywhere, any velocity measured is equal to an error in the velocity.

‡ For $h = 1/16$ results are identical for both methods. This is due to the fact that hardly any corrections need to be performed for this mesh, as the displacement of the interface is very small in the relation to the mesh width.

4.2. *Regularization of the corrections*

The analysis of the previous section indicates that local corrections to the LS function introduce undesirable errors in the curvature. A possible improvement would be to regularize the corrections and retain a smooth spatial representation of the curvature.

In the current method, the surface tension force is treated as a volume force. This requires the curvature to be computed in a small 'band' surrounding the interface. The curvature is defined as the divergence of the normal vector to the interface (equation 2.6). To compute a valid representation of the curvature in a region surrounding the interface, the gradient of the corrected LS function should be constant along the direction normal to the interface. Therefore, the first step in the proposed regularization procedure is to extend the local corrections, defined $\delta\phi = \phi^{n+1} - \phi^*$, along the direction normal to the interface by solving the following equation in pseudo-time τ:

$$\frac{\partial \delta\phi}{\partial \tau} + S(\phi^*)\frac{\nabla\phi^*}{|\nabla\phi^*|}\nabla\,\delta\phi = 0, \tag{4.2}$$

where $S(\phi^*)$ is the signum function defined:

$$S(\phi^*) = \begin{cases} -1 & \text{if } \phi^* < 0 \\ 0 & \text{if } \phi^* = 0 \\ 1 & \text{if } \phi^* > 0 \end{cases} \tag{4.3}$$

For numerical implementation of equation 4.2, a first order method is used as described in Peng, Merriman, Osher, Zhao & Kang (1999).

In addition to the extension procedure, a filter is applied to smooth the corrections in the direction tangential to the interface. The following interpolation function is applied to the corrections, consecutively in each coordinate direction, to attenuate high-frequency components:

$$\hat{\delta\phi} = \frac{1}{16}\left(-\delta\phi_{+2} + 4\delta\phi_{+1} + 10\delta\phi + 4\delta\phi_{-1} - \delta\phi_{-2}\right), \tag{4.4}$$

with $\hat{\delta\phi}$ the filtered corrections.

After treating the initial correction with the additional extension and filtering procedures, modified corrections are obtained and added to the initial approximation of the LS function. Due to the regularization, the effect of the initial correction procedure is altered and equation 3.13 may not necessarily hold. Therefore, the local correction, extension and filtering procedures are repeated iteratively in the following test case.

In our test case, the LS function of a perturbed spherical interface:

$$\phi^* = R(1-\lambda) - \sqrt{x^2 + y^2 + (z/(1-\lambda))^2} \tag{4.5}$$

is corrected back to a spherical interface of radius R, whose VOF function is represented by ψ^{n+1}. The perturbation λ is proportional to the mesh width, $\lambda \propto h$, and of such magnitude that the maximum volumetric error in each computational cell k is approximately 10%, i.e. $\max|\psi_k^{n+1} - f(\phi_k^*, \nabla\phi_k^*)| \approx 0.1$. After each iteration cycle of the modified correction procedure, the maximum relative error in curvature:

$$\max_k \left| \frac{\kappa_k^{n+1} - \kappa_k^*}{\kappa_k^{n+1}} \right| \tag{4.6}$$

	Max. relative error κ			Relative mass error		
Mesh width	1/32	1/64	1/128	1/32	1/64	1/128
Local method	$7.87 \cdot 10^{-1}$	1.64	3.60	$4.77 \cdot 10^{-6}$	$2.77 \cdot 10^{-6}$	$1.24 \cdot 10^{-6}$
Regularized method	$2.48 \cdot 10^{-4}$	$3.67 \cdot 10^{-4}$	$7.89 \cdot 10^{-4}$	$6.08 \cdot 10^{-6}$	$1.85 \cdot 10^{-6}$	$9.17 \cdot 10^{-7}$

TABLE 2. Comparison of maximum relative curvature and relative mass errors for the local and regularized correction methods. For the latter, only results after 24 iterations are shown.

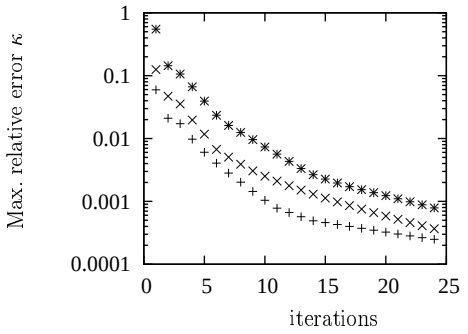

FIGURE 7. Maximum relative error in curvature as a function of iterations. (+) $h = 1/32$, (×) $h = 1/64$ and (∗) $h = 1/128$.

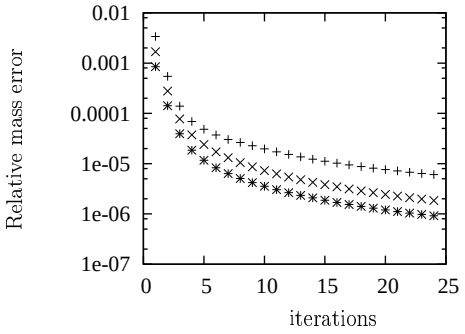

FIGURE 8. Relative mass error as a function of iterations. Symbols as in figure 7.

and the relative mass error

$$\frac{\sum_k \psi_k^{n+1} - f(\phi_k^{n+1}, \nabla\phi_k^{n+1})}{\sum_k \psi_k^{n+1}} \tag{4.7}$$

are computed and stored.

In table 2, results are compared of the local and regularized correction method, showing significant reduction of error in curvature for the new method. Figures 7 and 8 display successful convergence of errors with increasing number of iterations in case of the regularized method for each individual grid size. However, figure 7 also shows that for identical number of iterations, no convergence upon grid refinement is obtained for the maximum relative error in curvature. Furthermore, similar tests for less smoothly perturbed ϕ^* (not shown here) indicate unsatisfactory convergence of the mass error. Therefore actual implementation of the regularized correction procedure is not pursued.

5. Discussion

From the results presented in this work, we conclude that the coupling of LS and VOF interface descriptions by applying local corrections to the LS function should be avoided. The local corrections introduce non-smooth errors in the curvature and therefore surface tension force, because its computation involves second order derivatives of the LS function. As a result of these errors, spurious currents are enhanced, which limits the range of parameters (surface tension coefficient and viscosity) to be used for the

simulation of droplets. Moreover, the errors in surface tension force are shown to grow linearly upon grid refinement, which may affect the convergence and stability of the numerical method in general. Finally, the presented non-localization scheme is insufficient because, although it reduces the magnitude of the error in curvature, still does not guarantee convergence of the error upon grid refinement.

Instead, a global correction procedure could be applied, providing a LS function which is sufficiently smooth. Our proposition is to enforce two conditions on the LS function simultaneously:

$$\psi = f(\phi, \nabla\phi) \tag{5.1}$$

and

$$|\nabla\phi| = 1 \tag{5.2}$$

to obtain a mass conserving distance function to the piecewise linear interface. Currently, a variational LS method is considered, which reinitializes the LS function to accomplish equation 5.2 under the constraint for volume fraction, equation 5.1.

Although a priori estimation is difficult, a variational VOF/LS coupling procedure will be an additional effort in the code. Nonetheless, use of the LS function for the computation of the VOF advection has shown to be highly efficient in the MCLS code. Therefore, we still consider the combined VOF/LS approach an appropriate one to pursue.

Acknowledgments

Sander van der Pijl is greatly acknowledged for developing the MCLS method and providing us access to his code.

REFERENCES

Brackbill, J., Kothe, D. & Zemach, C. 1992 A continuum method for modeling surface tension. *J. Comp. Phys.* **100**, 335-354.

Chang, Y., Hou, T., Merriman, B. and Osher, S.1996 A level set formulation of Eulerian interface capturing methods for incompressible fluid flows. *J. Comp. Phys.* **124**, 449-464.

Loewenberg, M. & Hinch, E. J.1997 Collision of two deformable drops in shear flow. *J. Fluid Mech.* **338** 299-315.

Van der Pijl, S. P., Segal, A. & Vuik, C.2004 *Modeling of three-dimensional bubbly flows with a mass-conserving Level-Set method.* Proceedings European Congress on Computational Methods in Applied Sciences and Engineering, ECCOMAS 2004, Jyväskyä, Finland, July 24-28, 2004.

Van der Pijl, S. P., Segal, A., Vuik, C. & Wesseling, P.2004 A mass-conserving Level-Set method for modeling of multi-phase flows. *To appear in Int. J. Numer. Meth. Fluids.* http://ta.twi.tudelft.nl

Peng, D., Merriman, B., Osher, S., Zhao, H. & Kang, M.1999 A PDE-based fast local Level-Set method. *J. Comp. Phys.* **155**, 410-438.

Renardy, Y. & Renardy, M.2002 PROST: A parabolic reconstruction of surface tension for the Volume-of-Fluid method. *J. Comp. Phys.* **183**, 400-421.

SUSSMAN, M., SMEREKA, P. & OSHER, S.1994 A Level Set approach for computing solutions to incompressible two-phase flow. *J. Comp. Phys.* **114**, 146-159.

SUSSMAN, M. & PUCKETT, E. G.2000 A coupled Level Set and Volume-of-Fluid method for computing 3D and axisymmetric incompressible two-phase flows. *J. Comp. Phys.* **162**, 301-337.

Wang, H., Zinchenko, A. Z. & Davis, R. H.1994 The collision rate of small drops in linear flow fields *J. Fluid Mech.* **265**, 161-188.